RESEARCH PAPER

QbD based Formulation for Liposomal Combination of Adapalene-Clindamycin with Gel Matrix for Enhanced Acne Treatment

Hema[1], Anu Jindal[2], Shilpa[3], Onkar Bedi[4], Shubham Thakur[5], Thakur Gurjeet Singh[6], Amrinder Singh[7*]

[1,3,4,6,7] (Department of pharmacy, Chitkara University, Chitkara college of pharmacy, Rajpura, India)
(ranihema746@gmail.com) (shilpa82001@gmail.com) (onkar.bedi@chitkara.edu.in)
(gurjeet.singh@chitkara.edu.in) (amrinder.aulakh@yahoo.com)
[2] (Department of pharmacy, GHG Khalsa college of pharmacy, Gurusar Sadhar, Punjab, India)
(anumahajan78@gmail.com)
[5](Department of Pharmaceutics, ISF College of Pharmacy, Moga, Punjab, India)
(shubhamdthakur@gmail.com)

ABSTRACT

Background/Aim: The management of acne vulgaris often suffers from poor patient compliance due to topical irritation and low skin penetration. This study aimed to develop and optimize a Hyaluronic acid-Carbopol liposomal gel co-loaded with Adapalene and Clindamycin Phosphate to enhance topical delivery and therapeutic efficacy.

Methodology: Liposomal formulations were prepared using the thin-film hydration method and optimized via a 3-factor Box-Behnken design to evaluate the impact of lipid-to-cholesterol ratios on vesicle size and entrapment efficiency. The optimized formulation was characterized for particle size, polydispersity index, zeta potential, and drug encapsulation. *In vitro* release, *ex vivo* skin permeation (Franz diffusion cells), histopathological safety, and *in vivo* anti-acne efficacy were systematically evaluated.

Results: The optimized nano-liposomal gel exhibited a vesicle size of 165-170nm, a low polydispersity index, and a stable zeta potential of -31.1mV. *In vitro* studies confirmed sustained, diffusion-controlled drug release adhering to the Higuchi kinetic model. *Ex vivo* permeation demonstrated significant deeper skin penetration of both drugs compared to commercial formulation. Furthermore, the integration of Hyaluronic acid markedly improved skin hydration, collagen synthesis, and tissue elasticity. *In vivo* evaluation confirmed superior anti-acne efficacy with excellent skin tolerability.

Conclusion/ Originality: This study successfully reports the first Box-Behnken design-optimized, Hyaluronic acid-Carbopol liposomal gel co-loaded with Adapalene and Clindamycin phosphate. The developed system offers a promising, non-irritating, and high-penetration topical strategy that could significantly lower dosing frequency and improve patient compliance in acne therapy.

Keyword: Adapalene, Clindamycin phosphate, Liposomal gel, Box-Behnken design, Hyaluronic acid, Topical delivery**.**

How to cite this article: Hema, Jindal A, Shilpa, Bedi O, Thakur S, Singh TG, Singh A. QbD based Formulation for Liposomal Combination of Adapalene-Clindamycin with Gel Matrix for Enhanced Acne Treatment. Int J Drug Deliv Technol. 2026;16(59s): 1431-1444. DOI: 10.25258/ijddt.16.59s.161

Source of support: Nil

Conflict of interest: None

INTRODUCTION

Acne vulgaris is a chronic inflammatory skin disorder which affects the pilosebaceous unit, driven by *Propionibacterium acnes* (*P. acnes*) colonization, increased production of sebum, and accumulation of uneven skin cells of hair follicles [1, 2]. The *P. acnes* initiate the immune response characterized by the release of pro-inflammatory cytokines like TNF-α and interleukin 1β (IL-1β) which further leads to follicular inflammation and comedones formation [3, 4, 5, 6, 7]. The first line therapeutic regimens frequently employ combination therapies to concurrently target bacterial proliferation and inflammation. Notably, the combination of a topical retinoids, Adapalene (ADP), and a macrolide antibiotics, Clindamycin Phosphate (CLD)- such as the commercial formulation Deriva®-CMS is widely prescribed. However, these topical therapies are severely limited by poor skin absorption and notable adverse reactions like burning sensation, itching and redness [8, 9] which significantly compromise patient compliance. The other options then retinoids are

hormonal therapy or oral antibiotics, are often constrained by risk of reducing adrenal hormone [10], destroy gut bacteria and leads to antibiotic resistance [11, 12]. Consequently, there is an imperative need for novel, biocompatible topical drug delivery systems that optimize therapeutic outcomes while minimizing skin irritation [13, 14].

Liposomal vesicular systems offer a promising strategy to mitigate topical toxicity and enhance drug bioavailability. Composed of lipid bilayer capable of encapsulating hydrophobic molecules and an aqueous core for hydrophilic agents, liposomes eliminate the vesicle-induced toxicity common to conventional treatments. Furthermore, positively charged vesicles utilize the Donnan membrane effect to electrostatically adhere to the negatively charged stratum corneum, thereby promoting sustained, site-specific drug localization. To further augment therapeutic performance, hyaluronic acid (HA) can be integrated into the gel matrix. Celebrate for its unique viscoelastic properties, HA serves as a natural hydrating agent that stimulates collagen synthesis, improves ski elasticity, and accelerates tissue regeneration [15, 16, 17, 18, 19].

In this study, a dual-drug-loaded liposomal system was developed by encapsulating ADP and CLD within Phosphatidylcholine vesicles, which were subsequently incorporated into a hybrid HA-Carbopol 934P gel base to combine the moisturizing efficacy of HA with the synergistic antimicrobial and anti-inflammatory activities of the drugs [20]. A Quality-by-Design (QbD) approach utilizing Design of Experiments (DoE) was executed to systematically evaluate and optimize critical formulation variables. The optimized liposomal gel was comprehensively evaluated and compared against the commercial formulation via *in-vitro* release kinetics, *ex-vivo* transdermal permeation profiles, and *in-vivo* cutaneous irritation and anti-acne efficacy studies [21, 22, 23, 24, 25]. To the best of our knowledge, this is the first study reporting a HA-Carbopol-based liposomal gel co-loaded with ADP and CLD, optimized via Box-Behnken design (BBD), integrating enhanced dermal penetration with sustained drug release for optimized acne therapy.

MATERIALS AND METHODS

Materials

The ADP, CLD, and HA were gifted by Smayan Healthcare Pvt. Ltd. (Chandigarh, India). Soya Lecithin, brought from Hi Media. Chloroform was obtained from Merck (Mumbai, India). Cholesterol was purchased from SDFCL, and Carbopol 934P from Lubrizol. All other reagents were of analytical grade plus distilled water was generated in-house.

Ethical Statement

Preclinical experimental protocols were approved by the Institutional Animal Ethics Committee (IAEC) at Chitkara College of Pharmacy (Rajpura, Punjab, India) under the approval number IAEC/CCP/25/03/PR-03.

Formulation of ADP-CLD Liposomes

The thin film hydration technique was used for the formulation of liposomes [26, 27]. Briefly, ADP, CLD, cholesterol, and soya lecithin were dissolved in an organic phase of chloroform and methanol (7:3 v/v). The mixture was transferred to a round bottom flask (RBF) and evaporated using a rotary evaporator at 45 ^{o}C under reduced pressure (100rpm) until a thin film formed and then it is hydrated with 10 mL distilled water using the rotary evaporator (40 min, 100rpm). The resulting liposomal dispersion was sonicated at 25 ^{o}C for 20 min [28, 29, 30].

Box-Behnken Design (BBD) Optimization

Optimization was performed via Design-Expert® 13 software using a BBD. Independent variables evaluated at three levels included phospholipid (A), Cholesterol concentration (B), plus Probe sonication amplitude (C). The design generated 17 experimental runs (Table 1). Dependent responses selected for optimization were: Entrapment Efficiency of CLD (%EE of CLD), % Entrapment Efficiency of ADP (%EE of ADP), % and Vesicle size [31, 32, 33].

Table 1: Summary of independent and dependent variables and their levels in BBD

Independent variables (Factors)	**Unit**	**(-) Level**	**(+) Level**	**Dependent variables** (Responses)	**Unit**
A= Phospholipid	mM	10	20	Y1= % Entrapment Efficiency of CLD	%
B= Cholesterol	mM	5	20	Y2=% Entrapment Efficiency of ADP	%
C=Amplitude	%	40	60	Y3=Vesicle Size	Nm

Characterization of ADP-CLD Liposomes

Vesicle size, polydispersity index (PDI) and zeta potential, were determine using Zetasizer by diluting 10µL of the sample to 1mL with distilled water. Chemical compatibility was assessed via Fourier Transform Infrared (FTIR) spectrophotometry on lyophilized liposomal powder samples.

Differential Scanning Calorimetry (DSC)
DSC was used to analyze the thermal behavior of the drugs and excipients. The 2 mg of samples has been sealed in an aluminum pans and heated at a constant nitrogen flow rate (30mL/min). The thermal profiles were scanned from 30°C to 200°C for CLD and 30-400°C for ADP against an empty aluminum reference pan.

% Entrapment Efficiency (%EE)
The %EE was determine by separating unencapsulated drugs using a cooling ultracentrifuge (10,000 rpm, 15 min) at 4 °C. The concentration of free drug in the supernatant was quantified through validated HPLC system (Column: RP-C18, 150mm X 3.9, 5µm Waters). The mobile phase contains acetonitrile and 10 mM phosphate buffer (pH adjusted to 3.5 with orthophosphoric acid) at a 20:80 v/v ratio [34]. % EE was calculated using equation (1) [35]:

Efficiency of encapsulation = $[(C_t-C_f)/C_t] * 100$ (1)
Where, C_t = total drug concentration & C_f = concentration of the free drug.

Transmission Electron Microscopy (TEM)
TEM was used to examine vesicle morphology in which a single drop of the optimized formulation which placed on the copper grid covered with carbon, negatively stained with 1% w/v aqueous Phosphotungstic acid, and imaged at an accelerating voltage of 80kV.

Preparation of Liposomal Gel Formulations
Two distinct gel matrices were developed to evaluate the hydration benefits of HA [36, 37, 38, 39].

1. Carbopol base: Carbopol 934P (0.5-2% w/v) was dispersed in 20 mL distilled water and for hydration it was kept in it for 24 hrs. The pH was adjusted to 6.8-7.5 using 1m NaOH, followed by mechanical stirring at 5000 rpm for 2 hrs to yield a clear gel.

2. HA-Carbopol base: HA (0.1% w/v) was incorporated into the pre-hydrated Carbopol base and homogenized at 1500-2000 rpm at room temperature.

To prepare the final liposomal gels, the optimized liposomal dispersion was incorporated drop wise into both bases in a 1:1 ratio under continuous stirring until homogeneous.

Characterization of the Liposomal Gel
The formulations were evaluated visually for color and homogeneity. For pH determination, 0.1gm of gel was dissolved in 10 mL distilled water and measured using a calibrated pH meter (standardized at pH 4, 7, and 9) [24]. Rheological properties were assessed using a rotational viscometer equipped with an L-4 spindle (50 rpm, 20 gm sample, 5 min equilibration). Spreadability was measured via the parallel glass slide method using equation 2 [40]:
S = (M/ L)*T (2)
Where, S =Spreadability, M =Weight upon the upper slide (20 gm), L =length of the glass (7.5cm), and T= time (sec).

To determine % drug content, 1gm of gel was mixed in 100 mL methanol, filtered through Whatman Grade 41 paper, and quantified via the validated HPLC method using equation (3) [24]:

% Drug content = Free drug into gel/total drug into gel*100 (3)
Structural investigation and functional group integrity has been confirmed via FTIR spectroscopy [41].

***In-Vitro* Drug Release Assessment**
In vitro drug release kinetics has been assessed by Franz diffusion cell equipped with a dialysis membrane (pre soaked overnight in 40% ethanol) separating the donor and receptor compartment. The donor section was charged with 1 gm of either the control gel or liposomal gel; while the receptor compartment contains PB (pH 7.4).The system was maintained at 37±0.50°C under continuous magnetic stirring (100 rpm). At predetermined intervals (0.25, 0.5, 1, 2, 3, 4, 6, 8, 10, 12, and 24 hrs), 1 mL samples has been taken from the receptor medium and analyzed via HPLC. An equal volume of fresh buffer of pH 7.4 was added to maintain sink conditions [42].

***Ex-Vivo* Dermal Permeation Studies**
Cutaneous distribution and transdermal permeation were evaluated using excised, full-thickness, cleaned, and defatted mice skin mounted on modified Franz diffusion cell. The stratum corneum faced the donor chamber, and the dermis faced the receptor phase (25 mL PB, pH 7.4). A 0.5 gm gel dose (equivalent to 1mg ADP and 10.6 mg CLD) of either Sample 1 (HA-integrated liposomal gel) or Sample 2 (commercial Deriva®-CMS gel) has been applied to the donor chamber. The cells were stirred continuously at 37.0 ± 1.0°C. Aliquots were sampled at 1, 2, 3, 6, 12, 18, 24, 48, and 72 hrs, replaced instantly with fresh medium, and quantified via HPLC [43].

***In-Vivo* Skin Irritation Evaluation**

The irritation potential was assessed using Swiss albino mice with shaved dorsal skin (monitored for 24 hrs post-clipping to exclude injury-induced artifacts). Mice were randomly divided into four cohorts: Group I (2% NaOH; positive control), Group II (commercial Deriva®-CMS gel), Group III (ADP-CLD Carbopol liposomal gel), and Group IV (ADP-CLD-HA Carbopol liposomal gel). Test formulations (1 gm) were applied uniformly over a 2 cm^2 area. Cutaneous reactions (erythema and edema) was graded visually at 24, 48, and 72 hrs on a scale from (0) no response to (4) severe erythema/edema to calculate the Primary Irritation Index (PII) [44, 45].

***In-Vivo* Anti-Acne Efficacy**

Swiss Albino mice (20-30 gm) has been seprated into five groups (n=6): Group I: Normal control; Group II: Diseased control; Group III: Commercial Deriva®-CMS gel; Group IV: ADP-CLD Carbopol liposomal gel; and Group V: ADP-CLD-HA Carbopol liposomal gel. Following dorsal hair removal, acne was induced in Groups II-V via daily topical application of 2% ethanolic testosterone solution for 3 weeks. Following confirmation of sebaceous gland hypertrophy, treatments (0.1 gm/ 4 cm^2) were applied topically once daily for 2 weeks [46]. Acne severity and therapeutic reduction were quantified using the James and Tisser grading system [47].

RESULTS AND DISCUSSION

Pre-Formulation and Physiochemical Characterization

The optimized anti-acne liposomal gel exhibited off-white, translucent appearance with a highly homogenous, uniform consistency. Initial pre-formulation DSC thermograms identified sharp endothermic melting peaks for pure ADP and CLD at 328.30°C and 100.90°C, respectively. Shake flask partition coefficient (log P) values were determine to be 8.02 ±0.00 for ADP and 0.52±0.004 for CLD. Solubility profiling shows high ADP solubility in chloroform, methanol and ethanol, while CLD has optimal solubility in aqueous medium (water and PB at pH 7.4 and 6.8) and methanol. Consequently, a binary solvent system of chloroform and methanol (7:3 v/v) was selected as a organic phase in thin film hydration.

FTIR spectroscopy verifies the chemical identity and purity of both active pharmaceutical ingredients. The ADP spectrum displayed characteristic bands at 28848.30 cm^{-1} (O-H stretching), 1688.43 cm^{-1} (C=O stretching), 1475.50 cm^{-1} (C=C stretching) and 1303.10 cm^{-1} (C-O stretching). The CLD spectrum exhibited prominent peaks at 1678.35 cm^{-1} (C=O (carbonyl) stretching), 1456.97 cm^{-1} (O-H stretching/ bending), 1320.10 cm^{-1} (P=O stretching) and 1048.31 cm^{-1} (C-O stretching). The preservation of these diagnostic functional bands confirmed the structural integrity and purity of both drugs [48, 49].

Statistical Optimization via BBD

Numerical optimization was executed via Design-Expert® 13 software to achieve a maximized desirability score of 1.0. Constraints were applied to independent variables (Phospholipids: 10-20mM; Cholesterol: 5-20 mM; Amplitude: 40-60%) to optimize the target responses. The optimized constraints yielded a target transdermal permeation range of 84.02% to 97.275% for ADP and 81.86% to 96.83% for CLD, alongside a controlled viscosity range (11,159 -24,055 cP) and optimal spreadability (5.87 -19.97 gm*cm/sec). A final optimized batch composition is summarized in Table 2.

Table 2: Optimized composition of the dual-drug liposomal gel

Ingredients	Concentration
Adapalene / Clindamycin Phosphate	2.5mM / 25mM
Hyaluronic Acid / Carbopol	0.1% w/v / 1.0% w/v
Phospholipid / Cholesterol	20mM / 20mM
Chloroform: Methanol	7:3 v/v

The matrix of 17 experimental runs generated by BBD, along with corresponding dependent responses and PDI values, is summarized in Table 3. All formulations presented visually as stable, translucent, and aggregate-free dispersions.

Table 3: BBD layout with observed experimental responses

F-Code	Independent variables			Dependent variable			PDI
	Factor 1: Lipid (mM)	Factor 2: Amount of Cholesterol (mM)	Factor 3: Amplitude (%)	Response 1: %EE of CLD	Response 2:%EE of ADP	Response 3:Vesicle Size(nm)	

D1	10	5	50	69.55	44.81	450.25	0.236±0.005
D2	20	5	50	67.09	90.31	651.87	0.372±0.004
D3	10	20	50	83.72	90.14	210.82	0.115±0.004
D4	20	20	50	91.61	96.16	168.59	0.134±0.005
D5	10	12.5	40	64.81	66.8	420.64	0.377±0.007
D6	20	12.5	40	60.39	92.29	565.18	0.410±0.004
D7	10	12.5	60	60.33	66.78	493.64	0.345±0.004
D8	20	12.5	60	70.13	92.82	508.25	0.325±0.003
D9	15	5	40	66.13	68.46	569.97	0.354±0.006
D10	15	20	40	89.46	90.06	203.92	0.137±0.006
D11	15	5	60	72.68	65.25	572.56	0.368±0.003
D12	15	20	20	88.02	93.92	216.22	0.122±0.003
D13	15	12.5	50	89.43	92.12	385.28	0.382±0.004
D14	15	12.5	50	89.38	91.12	385.25	0.375±0.004
D15	15	12.5	50	89.26	92.28	386.43	0.366±0.004
D16	15	12.5	50	89.46	91.11	388.21	0.395±0.004
D17	15	12.5	50	89.21	91.81	388.35	0.374±0.003

Response Surface Analysis and Polynomial Modeling

Impact on % EE of ADP

The influence of variables on ADP entrapment followed a quadratic model (F-value = 2079.90, $p < 0.0001$), expressed via the coded polynomial equation 4.

% EE of ADP= $91.69+12.88A+12.68B+0.15C-9.87AB+0.14AC+1.77BC-5.54A^2-5.79B^2-6.47C^2$ (4)

The positive coefficients of phospholipid (A) and cholesterol (B) confirm that increasing lipid concentrations significantly enhances lipophilic ADP entrapment due to improved bilayer rigidity and surface area. Sonication amplitude (C) exerted a negligible linear effect. The negative interactive term (AB) and quadratic terms indicates a nonlinear optimization curvature, suggesting membrane saturation beyond optimal concentration.

Impact on % EE of CLD

The quadratic model for CLD entrapment was highly significant (F value = 35,753.66, $p < 0.0001$), yielded the coded equation 5:

% EE of CLD = $89.35+1.35A+9.67B+1.30C+2.59AB+3.56AC-2.00BC-13.26A^2+1.90B^2-12.18C^2$ (5)

Cholesterol content (B) exerted the primary positive effect on hydrophilic CLD entrapment, enhancing bilayer stability and preventing aqueous drug leakage. Phospholipid (A) and sonication amplitude (C) both displayed positive linear coefficients, while the interactive parameters indicated synergistic effects for AB and AC, coupled with an antagonistic response for BC.

Impact on Vesicle Size

The by quadratic relationships governing final particle size (F–value = 27,642.27, $p < 0.0001$) are defined by the coded equation 6:

Vesicle Size = $386.70+39.82A-180.64B+3.87C-60.96AB-32.48AC+2.43BC+44.97A^2-61.29B^2+65.25C^2$ (6)

The strong positive coefficient of phospholipid (A) tracks with the increased lipid content forming larger multi-lamellar architectures. Conversely, cholesterol (B) exhibited a strong negative effect, reflecting tighter lipid packing geometries and enhanced membrane rigidity that systematically reduced the final hydrodynamic diameter. The 3D response surface plots showing the impact on CLD and ADP entrapment efficiency, as well as liposomal vesicle size (Figure 1).

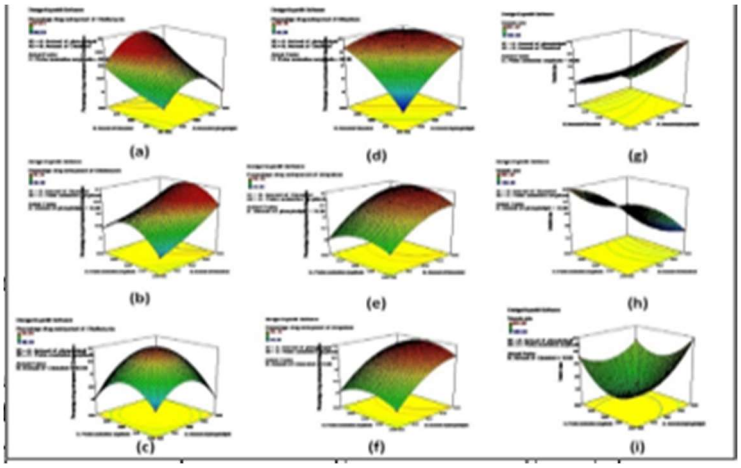

Figure 1: 3D Response surface plot of % EE of CLD (a,b,c) & ADP (d,e,f) and particle size (g,h,i) in liposomes (AB), (BC) & (AC)

Evaluation of the Numerically Optimized Solution

The software identified an optimized formulation (D18) achieving a perfect desirability score of 1.0. The experimental values closely matched the predicted values, demonstrating excellent homogeneity (PDI: 0.134) and an optimal balance between minimal vesicle size and maximum drug entrapment (Table 4).

Table 4: Optimized formulation parameters and predicted responses

Code	Phospholipid (mM)	Cholesterol (mM)	Amplitude (%)	%EE CLD (%)	%EE ADP (%)	Vesicle size (nm)	Desirability
D-18	13.84	19.58	49.16	98.60	97.17	167.47	1

Evaluation of Liposomes

Prior to the lypophilization process, visual monitoring of all formulations (D1-D17) verified their physical stability, maintaining off-white, translucent, and homogenous dispersion without phase separation or aggregate formation. Across all formulations, vesicle size ranged from 167.47 to 651.87 nm, while %EE for CLD was 60.33±0.13 to 91.61±0.42 and %EE for ADP was 44.81±0.36 to 96.16±0.01.

DSC Analysis

DSC thermograms (Figure 2) were used to evaluate the physical state of the encapsulated drugs. The pure active ingredients exhibited sharp crystalline endothermic melting peaks. Conversely, the selected formulation shows a shifted onset temperature at 316.74°C, with a complete absence of the characteristic crystalline peaks of pure drugs. This transition indicates that both therapeutic agents were successfully converted into an amorphous or molecularly dispersed state within the lipid matrix. The absence of extraneous thermal peaks further confirms excipients compatibility and system stability.

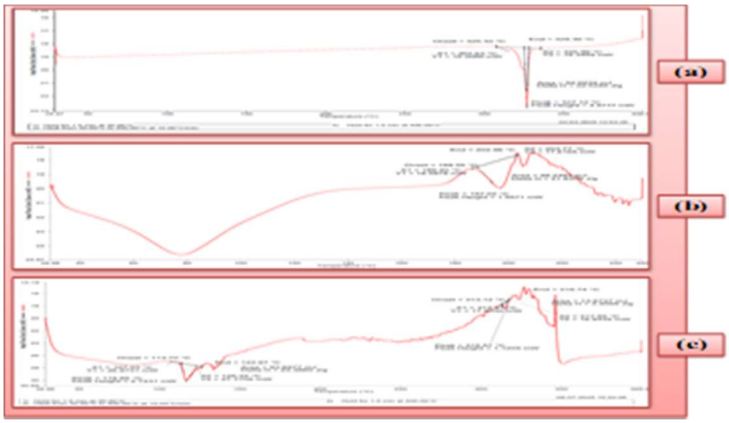

Figure 2: DSC of drugs (a) ADP & (b) CLD and (c) Optimized formulation

Vesicle Size and Surface Charge Analysis

The optimized ADP-CLD liposomal system exhibited an average hydrodynamic vesicle size of 164.63±0.80nm and having a low PDI of 0.258±0.007, confirming a narrow, uniform particle size distribution. The zeta potential was found to be -31.1 mV and due to the electrostatic repulsion between adjacent vesicles it indicating robust physical stability (Figure 3a).

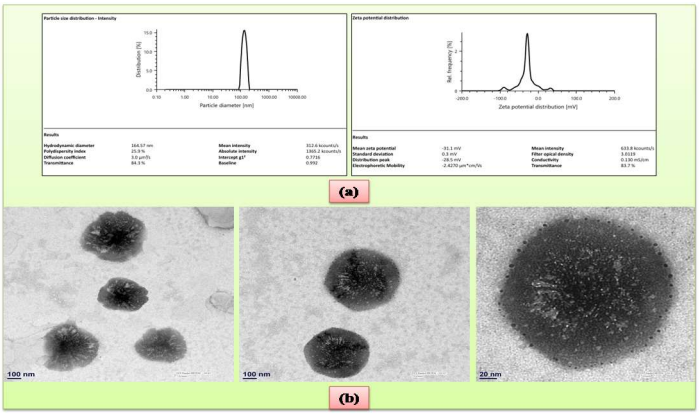

Figure 3: (a) Particle size and zeta potential of the optimized liposome powder, (b) TEM image of liposomes powder of optimized formulation at different scale

TEM Evaluation

TEM imaging (Figure 3b) demonstrated that vesicles have a distinct, uniform spherical morphology. This uniform spherical architecture maximizes drug loading capacity, prevents vesicle fusion or aggregation, and facilitates deep dermal penetration for enhanced therapeutic uptake.

FT-IR Spectroscopy Analysis

FT-IR spectra were analyzed to evaluate the chemical compatibility of the optimized D-18 formulations (Figure 4). The spectrum of the final formulation showed characteristic bands at 3396.20 cm^{-1} and 2848.21 cm^{-1} (O-H stretching of cholesterol), 168.96 cm^{-1} (C=O stretching of ADP), 1463.97 cm^{-1} (CH_3-CH_2 vibrations of cholesterol) and 1054.55cm^{-1} (C-O stretching of CLP). The preservation of these principle functional bands, coupled with a slight reduction in peak intensities and minor shifting, confirmed successful drug encapsulation within the liposomal core/bilayer. The complete absence of unexpected new peaks or major shifts rules out chemical incompatibilities or structural degradation.

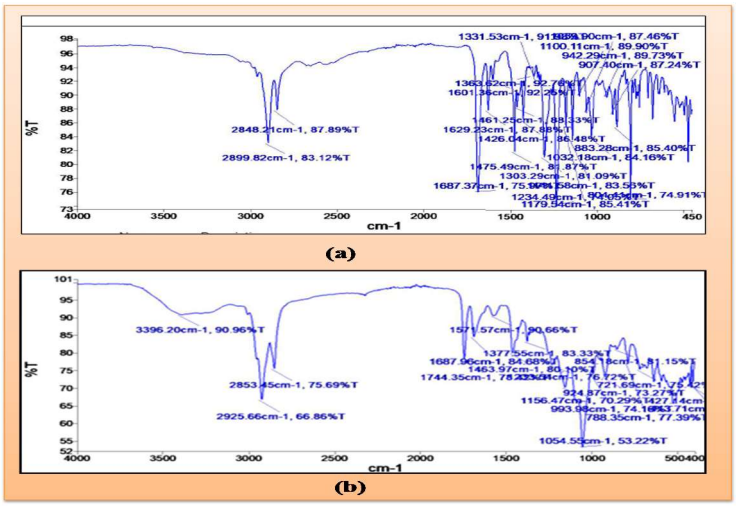

Figure 4: (a) FTIR of physical mixture of ADP, CLD, & Excipients; (b) FTIR of liposomes powder of optimized formulation

Characterization of the Liposomal Gel

Lyophilized liposomal powder was successfully dispersed into a Carbopol 934P gel matrix (0.5 to 2.0 % w/v) containing 0.1 % w/v of HA. Among the evaluated vesicle variations, formulation batch G2 (comprising 1.0 % w/v Carbopol 934P) was selected as optimal. It displayed ideal cutaneous physicochemical properties, including a skin compatible pH of 6.84, an optimal dynamic viscosity of 15,591 cPs, plus spreadability of 12.89gcm/sec. G2 also maintained high final drug content uniformities, yielding entrapment metrics of 97.27±4.45% for ADP and 96.83±0.81% for CLD. The structural rheology was directly controlled by the 1.0% w/v Carbopol network, which established 3D cross linked matrix that successfully balanced spatial gel stability with ease of topical application. The integration of 0.1% HA further augmented the system by providing localized hydration and improving structural skin retention.

***In-Vitro* Drug Release**

Comparative *in-vitro* release study revealed several limited drug release from the control gels, with only 29.53 % of ADP and 39.57 % of CLD. Conversely, the liposomal gel demonstrated significantly enhanced, biphasic diffusion kinetic with a broad 80 % release average across batches (Figure 5). The optimized G2 liposomal gel demonstrated the superior release profile, achieving a near-complete cumulative release of 97.09% for ADP and 96.14% of CLD within 24hrs timeframe. This enhanced profile is driven by vesicular solubilization and controlled lipid bilayer diffusion. This sustained release pattern maintains a prolonged concentration of both therapeutic agents at the pilosebaceous site, effectively minimizing required application frequencies and improving patient compliance

.

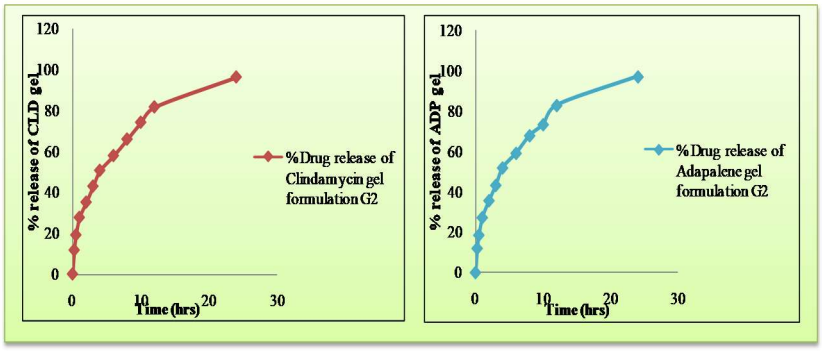

Figure 5: Percent drug release study of ADP-CLD-HA Carbopol liposomal gel

Drug Release Kinetics

To determine the precise drug transport mechanism, the cumulative release profiles of the optimized G2 formulation were mathematically adjusted to Zero-orders, First-order, Higuchi and Korsmeyer-Peppas models (Figure 6). The release data for both encapsulated drugs fit the Higuchi square- root model, yielding superior correlation coefficients ($R^2 \approx 0.997$; Table 5). This confirms a strictly matrix-diffusion-controlled transport mechanism. Additionally, the Korsmeyer-Peppas diffusional exponent ($n \approx 0.45$) indicates Fickian diffusion, verifying that the dual-loaded lipid bilayer enable steady, and prolonged drug delivery ideal for maintaining consistent therapeutic levels at the target site.

Table 5: Kinetic modeling and correlation coefficients (R^2) for optimized formulation (G2)

F- Code G2	Zero order		First order		Higuchi		K. Peppas	
	K_0	R^2	K_1	R^2	K_H	R^2	K_{KP}	R^2
ADP	3.6943	0.7643	-0.0453	0.9709	7.9629	0.997	0.4589	0.9863
CLD	3.5988	0.7637	-0.0412	0.9581	7.7718	0.997	0.453	0.9839

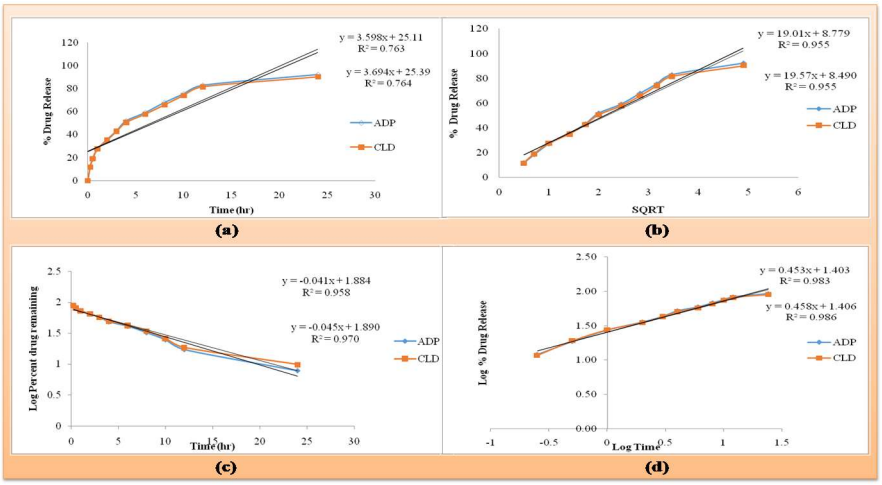

Figure 6: (a) Zero order, (b) Higuchi order, (c) First order, and (d) Korsmeyer-Peppas

***Ex-Vivo* Assessment of Liposomal Gel Performance**

Ex-vivo transdermal permeation profiling revealed a massive increase in cutaneous drug distribution from the optimized G2 liposomal gel compared to conventional commercial formulation (Figure 7). After 72-hrs, the cumulative permeation from G2 reached 486µg/cm² for ADP and 473.06µg/cm²for CLD. In contrast, the commercial gel showed significantly lower retention metrics, yielding only 118.07±0.479µg/cm² for ADP and 120.197±0.174µg/cm² for CLD. Furthermore, G2 demonstrated superior permeation coefficients (K_p = 0.6710 cm/hr for ADP and 0.0636 cm/hr for CLD) compared to the commercial gel (0.014 cm/hr for ADP and 0.010 cm/hr for CLD). This marked increase in interacting electrostatically and biochemically with the lipid matrix of the stratum corneum, allowing deep follicular penetration and localized drug retention.

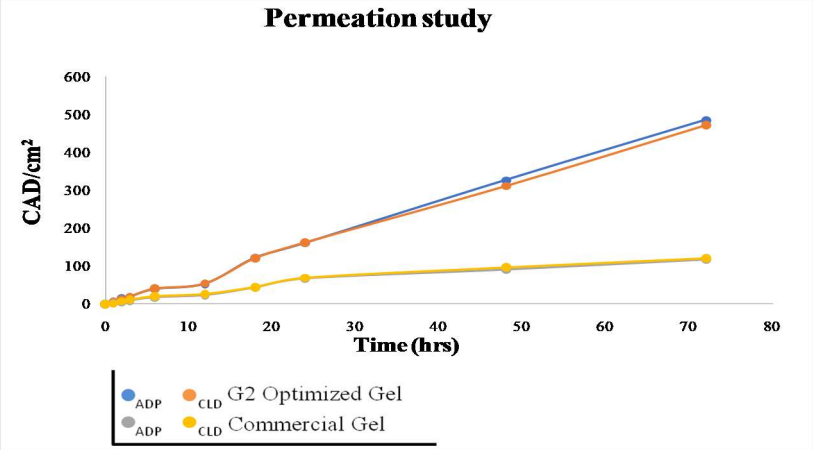

Figure 7: *Ex vivo* drug permeation of liposomal gel and commercial gel

***In-Vivo* Cutaneous Irritancy Assessment**

The cutaneous tolerance of the formulations was evaluated over 72 hrs in mice models using a visual scoring method. The developed dual-drug-loaded liposomal gel caused minimal to no erythema or cutaneous changes. The computed Primary Irritation Index (PII) scores (Table 6) verified that both liposomal formulations (Group III and IV) possessed and identical, exceptionally low PII of 0.17- far below the baseline irritation threshold (PII<1.0). Conversely, the commercial gel reference (Group II) yielded a higher PII score of (~ 0.3), while the positive control (2% NaOH; Group I) generated a massive PII score of 2.00.these metrics confirms that the lipid vesicular matrix and the HA-Carbopol base establish a biocompatible topical system that shields skin tissues from direct retinoid-induced contact irritation [50].

Table 6: PII scores across experimental cohorts

Cohort (n=6)	Time			PII (Score/n)	Irritancy Classification
	24hr	48hr	72hr		
Group I	4	4	4	02	Severe irritant
Group II	0	1	1	0.3	Negligible/Mild
Group III	0	1	0	0.17	Negligible/Safe
Group IV	0	0	1	0.17	Negligible/Safe

(n= no. of animals in each group)

***In-Vivo* Anti-Acne Efficacy and Histopathology**

Topical induction using a 2% ethanolic testosterone for 28 days successfully induced Grade 3 acne lesions in female Swiss albino mice. Following a 7- day treatment cycle, the cohorts showed clear variations in therapeutic response (Figure 8). The commercial gel (Group III) achieved partial remediation, downscaling lesion severity to Grade 2. The standard ADP-CLD Carbopol liposomal gel (Group IV) accelerated clearance to Grade 1. Most notably, the hybrid ADP-CLD-HA Carbopol liposomal gel (Group V) pushed lesion clearance below Grade 1, achieving complete therapeutic resolution.

Histopathological tracking corroborated the macroscopic scores. While the commercial reference yielded incomplete follicular restricting and retained minor inflammatory infiltrates, the plain liposomal gel (Group IV) significantly resolved dermal inflammation and regularized the epidermis. The optimized HA-enriched liposomal gel (Group V) demonstrated complete tissue recovery, reconstructing near-normal ski morphology, minimizing sebaceous gland hypertrophy, and yielding superior localized collagen bundle architecture.

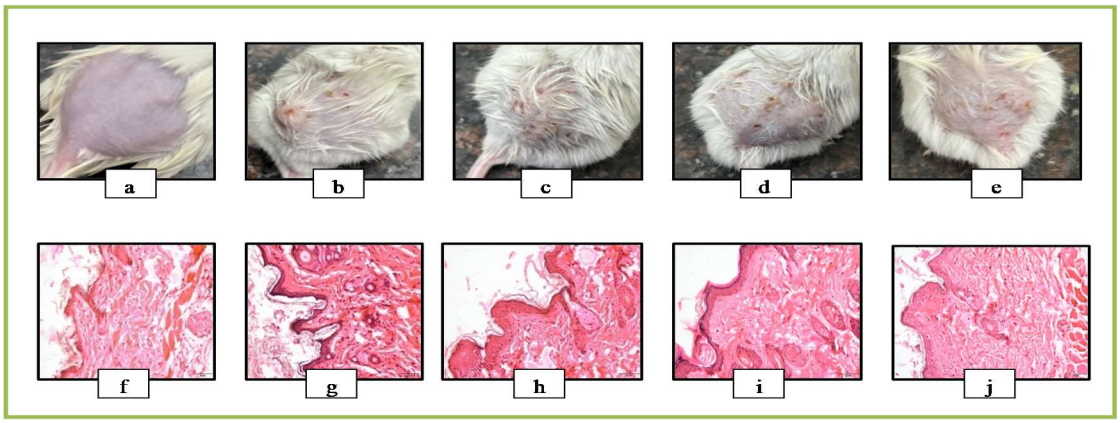

Figure 8: Macro-photographic and histopathological tracking of *in-vivo* anti-acne efficacy. Gross anatomical skin profiles after a 7-day therapeutic cycle showing: **(a)** Normal control, **(b)** Diseased untreated control (Grade 3 acne), **(c)** Commercial gel reference, **(d)** ADP-CLD Carbopol liposomal gel, and **(e)** Optimized ADP-CLD-HA Carbopol liposomal gel. Corresponding H&E stained cutaneous histopathology sections showing: **(f)** Normal baseline tissue architecture, **(g)** Testosterone-induced acne showcasing sebaceous hypertrophy and follicular damage, **(h)** Partial structural remediation from commercial gel, **(i)** Marked reduction in dermal inflammation via plain liposomal gel, and **(j)** Complete tissue recovery with normalized skin morphology and organized collagen bundles via the HA-enriched liposomal gel

CONCLUSION

This study successfully developed and optimized a hybrid HA-based Carbopol gel matrix integrated with ADP and CLP –co-loaded liposomal gel for enhanced topical acne therapy. BBD optimization yielded stable, monodisperse, nanosized vesicles (~ 165-170nm) with a robust zeta potential (-31.1mV) that effectively maximized drug encapsulation while maintaining structural skin compatibility. *In vitro* diffusion kinetics followed a matrix-controlled Higuchi model, establishing a sustained release pattern ideal for reducing application frequencies. Furthermore, *ex-vivo* skin permeation profiling demonstrated significantly enhanced transdermal delivery and higher permeation coefficients compared to the commercial gel, driven by favorable vesicular lipophilic interactions with the stratum corneum. The integration of 0.1% w/v HA provided localized cutaneous hydration, stimulated collagen reorganization, and accelerated epidermal recovery. Ultimately, *in-vivo* evaluations confirmed that the dual-drug HA-Carbopol liposomal gel achieves superior lesion clearance, minimizes retinoid-induced skin irritancy, and outpaces conventional commercial formulations. This biocompatible topical delivery system represents a highly promising alternative for optimized acne management and warrants further clinical evaluations.

ACKNOWLEDGMENT

The authors are grateful to Smayan Healthcare Pvt. Ltd. (Chandigarh, India) for generously providing the gift samples of ADP, CLP, and HA utilized in this research.

CONFLICT OF INTEREST

The authors declare no conflict of interest associated with this study.

REFERENCES

1. Kurokawa I, Danby FW, Ju Q, Wang X, Xia L, Chen W, et al. New developments in our understanding of acne pathogenesis and treatment. Experimental Dermatology. 2009;18(10):821–832. DOI: 10.1111/j.1600-0625.2009.00890.x
2. Williams HC, Dellavalle RP, Garner S. Acne vulgaris. The Lancet. 2012;379(9813):361–372. DOI: 10.1016/S0140-6736(11)60321-8
3. Graham G, Farrar M, Cruse-Sawyer J, Holland KT, Ingham E. Proinflammatory cytokine production by human keratinocytes stimulated with Propionibacterium acnes and P. acnes GroEL. British Journal of Dermatology. 2004;150(3):421–428. DOI: 10.1046/j.1365-2133.2004.05762.x
4. Nagy I, Pivarcsi A, Kis K, Koreck A, Bodai L, McDowell A, et al. Propionibacterium acnes and lipopolysaccharide induce the expression of antimicrobial peptides and proinflammatory cytokines/chemokines in human sebocytes. Microbes and Infection. 2006;8(8):2195–2205. DOI: 10.1016/j.micinf.2006.04.001
5. Lee SE, Kim JM, Jeong SK, Jeon JE, Yoon HJ, Jeong MK, et al. Protease-activated receptor-2 mediates the expression of inflammatory cytokines, antimicrobial peptides, and matrix metalloproteinases in keratinocytes in response

to Propionibacterium acnes. Archives of Dermatological Research. 2010;302(10):745–756. DOI: 10.1007/s00403-010-1074-z
6. Jeremy AH, Holland DB, Roberts SG, Thomson KF, Cunliffe WJ. Inflammatory events are involved in acne lesion initiation. Journal of Investigative Dermatology. 2003;121(1):20–27. DOI: 10.1046/j.1523-1747.2003.12321.x
7. Freedberg IM, Tomic-Canic M, Komine M, Blumenberg M. Keratins and the keratinocyte activation cycle. Journal of Investigative Dermatology. 2001;116(5):633–640. DOI: 10.1046/j.1523-1747.2001.01327.x
8. Hsieh M, Chen C. Delivery of pharmaceutical agents to treat acne vulgaris: current status and perspectives. Journal of Medical and Biological Engineering. 2011;32(4):215–224. DOI: 10.5405/jmbe.901
9. Wang CH, Wang LK, Tsai FM. Exploring potential therapeutic applications of tazarotene: gene regulation mechanisms and effects on melanoma cell growth. Current Issues in Molecular Biology. 2025;47(4):237. DOI: 10.3390/cimb47040237
10. Tommasino N, Annunziata MC, Potestio L, Napolitano M. Efficacy and safety of hormonal therapies for acne: a narrative review. Clinical, Cosmetic and Investigational Dermatology. 2025;18:3331–3337. DOI: 10.2147/CCID.S574341
11. Adler BL, Kornmehl H, Armstrong AW. Antibiotic resistance in acne treatment. JAMA Dermatology. 2017;153(8):810–811. DOI: 10.1001/jamadermatol.2017.1297
12. Sinnott SJ, Bhate K, Margolis DJ, Rogers S, Smith SM. Antibiotics and acne: an emerging iceberg of antibiotic resistance? British Journal of Dermatology. 2016;175(6):1127–1132. DOI: 10.1111/bjd.15129
13. Aslam I, Fleischer A, Feldman S. Emerging drugs for the treatment of acne. Expert Opinion on Emerging Drugs. 2015;20(1):91–101. DOI: 10.1517/14728214.2015.990373
14. Leyden JJ. A review of the use of combination therapies for the treatment of acne vulgaris. Journal of the American Academy of Dermatology. 2003;49(3 Suppl):S200–S210. DOI: 10.1067/S0190-9622(03)01154-X
15. Makvandi P, Ali GW, Della Sala F, Abdel-Fattah WI, Borzacchiello A. Biosynthesis and characterization of antibacterial thermosensitive hydrogels based on corn silk extract, hyaluronic acid and nanosilver for potential wound healing. Carbohydrate Polymers. 2019;223:115023. DOI: 10.1016/j.carbpol.2019.115023
16. Pacini S, Punzi T, Gulisano M, Ruggiero M. Pulsed current iontophoresis of hyaluronic acid in living rat skin. Journal of Dermatological Science. 2006;44(3):169–171. DOI: 10.1016/j.jdermsci.2006.08.012
17. Makvandi P, Ali GW, Della Sala F, Abdel-Fattah WI, Borzacchiello A. Hyaluronic acid/corn silk extract based injectable nanocomposite: a biomimetic antibacterial scaffold for bone tissue regeneration. Materials Science and Engineering C. 2020;107:110195. DOI: 10.1016/j.msec.2019.110195
18. Neuman MG, Nanau RM, Oruña L, Coto G. In vitro anti-inflammatory effects of hyaluronic acid in ethanol-induced damage in skin cells. Journal of Pharmacy and Pharmaceutical Sciences. 2011;14(3):425–437. DOI: 10.18433/j3qs3j
19. Bukhari SNA, Roswandi NL, Waqas M, Habib H, Hussain F, Khan S, et al. Hyaluronic acid, a promising skin rejuvenating biomedicine: a review of recent updates and pre-clinical and clinical investigations on cosmetic and nutricosmetic effects. International Journal of Biological Macromolecules. 2018;120:1682–1695. DOI: 10.1016/j.ijbiomac.2018.09.188
20. Morrow DIJ, McCarron PA, Woolfson AD, Donnelly RF. Innovative strategies for enhancing topical and transdermal drug delivery. Open Drug Delivery Journal. 2007;1:36–59. DOI: 10.2174/1874126600701010036
21. Wasankar SR, Faizi SM, Deshmukh AD. Formulation and development of liposomal gel for topical drug delivery system. International Journal of Pharmaceutical Sciences and Research. 2012;3(11):4461–4470. DOI: 10.13040/IJPSR.0975-8232.3(11).4461-70
22. Değim Z, Çelebi N, Alemdaroğlu C, Deveci M, Öztürk S, Özoğul C. Evaluation of chitosan gel containing liposome-loaded epidermal growth factor on burn wound healing. International Wound Journal. 2011;8(4):343–354. DOI: 10.1111/j.1742-481X.2011.00795.x
23. de Castro MA, Reis PHL, Fernandes C, de Sousa RG, Inoue TT, Fialho SL, et al. Thermoresponsive in-situ gel containing hyaluronic acid and indomethacin for the treatment of corneal chemical burn. International Journal of Pharmaceutics. 2023;631:122468. DOI: 10.1016/j.ijpharm.2022.122468

24. Prakash A, Malviya R, Sridhar SB, Wadhwa T, Shareef J. Physicochemical properties, drug delivery, and tissue engineering applications of neem gum and its derivatives: a comprehensive review. Mini Reviews in Medicinal Chemistry. 2025;25. DOI: 10.2174/0113895575403808251008045503
25. Lodeiro IG, Macphee DE, Palomo A, Fernández-Jiménez A. Effect of alkalis on fresh C–S–H gels: FTIR analysis. Cement and Concrete Research. 2009;39(3):147–153. DOI: 10.1016/j.cemconres.2009.01.003
26. Zhang H. Thin-film hydration followed by extrusion method for liposome preparation. Methods in Molecular Biology. 2017;1522:17–22. DOI: 10.1007/978-1-4939-6591-5_2
27. Kumar V, Banga AK. Intradermal and follicular delivery of adapalene liposomes. Drug Development and Industrial Pharmacy. 2016;42(6):871–879. DOI: 10.3109/03639045.2015.1082580
28. Umbarkar M, Thakare S, Surushe T, Giri A, Chopade V. Formulation and evaluation of liposome by thin film hydration method. Journal of Drug Delivery and Therapeutics. 2021;11(1):72–76. DOI: 10.22270/jddt.v11i1.4677
29. Chauhan SB, Gupta V. Recent advances in liposome. Research Journal of Pharmacy and Technology. 2020;13(4):2051–2056. DOI: 10.5958/0974-360X.2020.00369.8
30. Singh A, Srivastava A, Gupta A. Liposomal drug delivery system – a review. Journal of Applied Pharmaceutical Science Research. 2020;3(3):7–10. DOI: 10.31069/japsr.v3i3.2
31. Kurmi BD, Paliwal SR. Development and optimization of TPGS-based stealth liposome of doxorubicin using Box–Behnken design: characterization, hemocompatibility, and cytotoxicity evaluation in breast cancer cells. Journal of Liposome Research. 2022;32(2):129–145. DOI: 10.1080/08982104.2021.1903034
32. Chaudhary H, Kohli K, Amin S, Rathee P, Kumar V. Optimization and formulation design of gels of diclofenac and curcumin for transdermal drug delivery by Box-Behnken statistical design. Journal of Pharmaceutical Sciences. 2011;100(2):580–593. DOI: 10.1002/jps.22292
33. Khute S, Jangde RK. Optimization of nasal liposome formulation of venlafaxine hydrochloride using a Box-Behnken experimental design. Current Therapeutic Research. 2023;99:100714. DOI: 10.1016/j.curtheres.2023.100714
34. Khatri RH, Patel RB, Patel MR. A new RP-HPLC method for estimation of clindamycin and adapalene in gel formulation: development and validation consideration. Thai Journal of Pharmaceutical Sciences. 2014;38(1):44–48. DOI: 10.56808/3027-7922.1969
35. Upadhyay DK, Sharma A, Kaur N, Gupta GD, Narang RK, Rai VK. Nanoemulgel for efficient topical delivery of finasteride against androgenic alopecia. Journal of Pharmaceutical Innovation. 2021;16:735–746. DOI: 10.1007/s12247-020-09483-9
36. Ribeiro M, Ferraz MP, Monteiro FJ, Fernandes MH, Beppu MM, Mantione D, et al. Antibacterial silk fibroin/nanohydroxyapatite hydrogels with silver and gold nanoparticles for bone regeneration. Nanomedicine. 2017;13(1):231–239. DOI: 10.1016/j.nano.2016.08.026
37. Donejko M, Przylipiak A, Rysiak E, Miltyk W, Galicka E, Przylipiak J, et al. Hyaluronic acid abrogates ethanol-dependent inhibition of collagen biosynthesis in cultured human fibroblasts. Drug Design, Development and Therapy. 2015;9:6225–6233. DOI: 10.2147/DDDT.S91968
38. Al-Halaseh LK, Al-Jawabri NA, Tarawneh SK, Al-Qdah WK, Abu-Hajleh MN, Al-Samydai AM, et al. A review of the cosmetic use and potentially therapeutic importance of hyaluronic acid. Journal of Applied Pharmaceutical Science. 2022;12(7):34–41. DOI: 10.7324/JAPS.2022.120703
39. Sharma T, Thakur S, Kaur M, Singh A, Jain SK. Novel hyaluronic acid ethosomes-based gel formulation for topical use with reduced toxicity, better skin permeation, deposition, and improved pharmacodynamics. Journal of Liposome Research. 2023;33:129–143. DOI: 10.1080/08982104.2022.2087675
40. Estanqueiro M, Amaral MH, Sousa Lobo JM. Comparison between sensory and instrumental characterization of topical formulations: impact of thickening agents. International Journal of Cosmetic Science. 2016;38:389–398. DOI: 10.1111/ics.12302
41. Saleh W, Abozaid D, Aljaiyash A, Ali A. Formulation and evaluation of a topical herbal gel containing Rosmarinus officinalis for anti-inflammatory activity. AlQalam Journal of Medical and Applied Sciences. 2026;:38–45. DOI: 10.54361/ajmas.269108

42. Salamanca CH, Barrera-Ocampo A, Lasso JC, Camacho N, Yarce CJ. Franz diffusion cell approach for pre-formulation characterisation of ketoprofen semi-solid dosage forms. Pharmaceutics. 2018;10(3):148. DOI: 10.3390/pharmaceutics10030148
43. Ghosh M, Roy D, Singh RP, Kurmi BD, Singh A. Novel hyaluronic acid-based adapalene nano vesicular formulation for enhanced anti-acne control: a sensitivity and pharmacodynamic analysis. Journal of Cluster Science. 2025;36(5):160. DOI: 10.1007/s10876-025-02886-z
44. Das S, Wong ABH. Stabilization of ferulic acid in topical gel formulation via nanoencapsulation and pH optimization. Scientific Reports. 2020;10(1):12288. DOI: 10.1038/s41598-020-68732-6
45. Varma VNSK, Maheshwari P, Navya M, Reddy SC, Shivakumar H, Gowda D. Calcipotriol delivery into the skin as emulgel for effective permeation. Saudi Pharmaceutical Journal. 2014;22:591–599. DOI: 10.1016/j.jsps.2014.02.007
46. Demurtas A, Nicoli S, Pescina S, Marchitto L, Ragni L, Russo V, et al. Development, optimization and ex-vivo evaluation of a transdermal formulation containing trazodone. European Journal of Pharmaceutical Sciences. 2024;201:106874. DOI: 10.1016/j.ejps.2024.106874
47. Kausar H, Mujeeb M, Ahad A, Moolakkadath T, Aqil M, Ahmad A, et al. Optimization of ethosomes for topical thymoquinone delivery for the treatment of skin acne. Journal of Drug Delivery Science and Technology. 2019;49:177–187. DOI: 10.1016/j.jddst.2018.11.016
48. Ramli R, Malik AS, Hani AFM, Jamil A. Acne analysis, grading and computational assessment methods: an overview. Skin Research and Technology. 2012;18:1–14. DOI: 10.1111/j.1600-0846.2011.00542.x
49. Sahoo S, Chakraborti CK, Mishra SC. Qualitative analysis of controlled release ciprofloxacin/carbopol 934 mucoadhesive suspension. Journal of Advanced Pharmaceutical Technology and Research. 2011;2(3):195–204. DOI: 10.4103/2231-4040.85541
50. Bae IH, Kwak JH, Na CH, Kim MS, Shin BS, Choi H. A comprehensive review of the acne grading scale in 2023. Annals of Dermatology. 2024;36(2):65–73. DOI: 10.5021/ad.23.09